

## **Response on RC2**

Thanks for your time and helpful feedbacks on our manuscript. We have addressed the comments and will implement the proposed changes in the manuscript. Please, see below our detailed response. General comments were responded to in paragraphs, and Specific Comments were responded to point by point.

Our response is highlighted in blue. We will provide a track-change version together with the revised paper.

### **General comments**

The authors have developed a method to map Arctic sea ice leads using Thermal Infrared Spectrometer (TIS) data onboard recently (Nov 2021) launched Chinese Sustainable Development Science Satellite 1 (SDGSAT- 1). TIS has three IR bands: B1 (8.0- 10.5  $\mu\text{m}$ ), B2 (10.3- 11.3  $\mu\text{m}$ ) and B3 (11.5- 12.5  $\mu\text{m}$ ), with 30 m resolution and 300 km swath width. The TIS instrument provides TIR data at much finer resolution than MODIS (1 km) and VIIRS (750 m), and somewhat finer than Landsat 8/9 (100 m). Optical and NIR data at comparable or even finer resolution are available from many sensors (e.g. Sentinel-2, Landsat 8/9), but only TIR data enables to retrieve sea ice properties regardless of daylight conditions.

The method for the Arctic sea ice leads mapping is developed using 11 TIS images acquired over the Laptev and Beaufort Seas in March and April 2022. The general lead detection method was same for all three TIS bands with some variable parametrization, i.e. all three bands were not used together for the lead detection, but in some cases the resulting three lead maps were combined (if I understood correctly, please see my comment later). The same TIS images were also processed to the leads maps (binary map: lead (open water or thin ice) or sea ice). The leads by the three TIS bands were compared to each other, and to lead detection maps by Sentinel-2 band 2 (green band) data and MODIS daily IST data. The Sentinel-2 lead detection was based on study by Muchow et al. (20121) and the MODIS lead detection to (Qu et al.

2021). A case study was also conducted where a TIS lead map was compared to Sentinel-1 dual-polarization SAR image. Possible atmospheric influences to the TIS lead detection were investigated using ERA5 air temperature and OMI ozone total column data. The TIS band 1 covers the ozone absorption band.

In general, the TIS lead detection seemed to work fine, and against the S-2 lead maps there was 96.3% pixel based match (authors used TIS accuracy here). Compared with the MODIS lead map, the TIS map presents more leads with width less than hundreds of meters. All three TIS bands showed similar performances in detecting leads. The B1 band can be complementary to the other two bands, as the temperature sensitivity is different from the other two, benefiting better detection by combining the three bands. Arctic lead maps with fine resolution (e.g. 30 m) allow to observe narrow leads which are undetected in the MODIS/VIIRS products, and estimate their contribution to the overall Arctic lead fraction.

I think the study set up with data acquisitions and data processing is rather well conducted, and the TIS lead detection method could be generally applicable for a large number of TIS images, but I think it is not sure as it is based on a small amount of data. Further, I don't think it is meaningful to develop lead detection methods for the three TIS bands separately, and compare the results. You should develop the best possible lead detection algorithm for the TIS data (having as input all bands or just two/one), and only present this in the paper. In the following I have also some other major comments to the papers and suggestions for possible improvements. These are followed by miscellaneous specific ones.

**Response:** Thanks for your valuable comment. We agree that it would be better to apply the most appropriate thermal infrared band for lead detection. However, until the cross-comparison experiments were carried out, we found each band has its advantage on ice leads detection.

The TIS three thermal infrared bands showed different radiometric accuracy during the commissioning phase. The absolute radiometric calibration evaluation by

Hu et al. (2022) suggested that the average temperature bias of SDGSAT-1 TIS reached 0.661 K, 1.081 K and 0.426 K for B1, B2 and B3, respectively. This suggests that the B3 band has the best radiometric calibration accuracy. However, B2 and B3 bands are more affected by the strip noise than the B1 band. B1 band is a less common thermal infrared channel with colder temperatures than the other two split-window channels (B2 and B3 bands) due to the absorption effect of ozone. Few studies have investigated its similarities and differences with the 11 and 12  $\mu\text{m}$  TIR channel for sea ice remote sensing. However, we do find that using the TIS B1 band can obtain more small leads in the presence of interference in B2 and B3 data.

Taken together, it is necessary to carry out a comprehensive application demonstration of the new on-board sensor. We applied the same method to the three bands of SDGSAT-1 TIS to extract leads, and further conducted cross-comparison to determine their detection performance. The cross-comparison results suggest it is beneficial to combine the lead detection results of the TIS three bands.

The review and discussion on related previous studies is well conducted, e.g. different methods for lead detection are nicely discussed. However, your review could include also following new study:

Q. Wang, M. Shokr, S. Chen, Z. Zheng, X. Cheng and F. Hui, "Winter Sea-Ice Lead Detection in Arctic Using FY-3D MERSI-II Data," in *IEEE Geoscience and Remote Sensing Letters*, vol. 19, pp. 1-5, 2022, Art no. 7005105, doi: 10.1109/LGRS.2022.3223689.

There are many studies with lead detection using SAR and altimeter data, and it is fine to give only few examples as you have done. Related to (Murashkin and Spreen, 2019) include also reference:

Dmitrii Murashkin, Gunnar Spreen, Marcus Huntemann, and Wolfgang Dierking, "Method for detection of leads from Sentinel-1 SAR images," *Annals of Glaciology*, vol. 59, no. 76, pp. 124–136, 2018

Could you use their method for automatic lead detection in your S-1 SAR imagery? This would allow better utilization of the SAR imagery as comparison data.

Your review includes only one study where Landsat data are used for the lead

detection (Qu et al. 2019). Are there any other Landsat studies? Please check. One relevant study here could be:

Cáceres, A.; Schwarz, E.; Aldenhoff, W. Landsat-8 Sea Ice Classification Using Deep Neural Networks. *Remote Sens.* 2022, 14, 1975. <https://doi.org/10.3390/rs14091975>

Sentinel-2 lead study by (Muchow et al. 2022) must be discussed in Introduction, it is now mentioned later in Section 4.1.

You could also summarize currently publicly available Arctic lead products with their time spans, seasonal coverages (full year or only winter season) and spatial resolutions.

**Response:** Thank you very much for your advice. We carefully checked relevant literatures and restructured the corresponding paragraphs in the Introduction section to better review recent studies. Table R1 shows the current publicly available Arctic lead datasets developed by different methods at different resolution with time spans, which will be added to the revised version.

It should be noted that the sea ice classification algorithm developed by Cáceres et al. (2022) based on Landsat-8 focuses on the different sea ice types (ice free, gray to white ice, thin first year ice and medium first year ice) in the Baltic Sea. No lead detection or observation is involved. Therefore, this paper is not cited.

In Section 5.2, the purpose of the comprehensive analysis incorporating Sentinel-1 data with the TIS detected results is to explore the property within the lead. For this purpose, we have specifically analyzed a complex scenario congaing a potential transition zone between thin ice and seawater, as shown in Figure 13 in the original manuscript. Although we did not use the automated S1 lead detection algorithm (Murashkin and Spreen, 2018), the S1 images in dual-polarization provide valuable backscatter information than a binary result. The backscatter of the lead transition zone, which is higher in the S1 HH image and lower in the HV image, was consistent with the “bright lead” feature described by Murashkin and Spreen (2018). However, the backscatter of surrounding ice is rather inhomogeneous and the contrast

with the lead is not significant in both the HH and HV images. Notably, Murashkin and Spreen (2018) did not analyze this situation. Therefore, the automated lead detection algorithm may not be adapted to the scenario we have shown here. In contrast, it is more appropriate to analyze the differences between HH and HV data directly, so we have performed a false-color composite using the dual-polarized data.

Table R1 Arctic lead datasets and with their spatial resolution and time span.

<b>Dataset</b>	<b>Satellite sensor</b>	<b>Spatial resolution</b>	<b>Time span and seasonal coverage</b>	
Bröhan and Kaleschke (2014)	AMSR-E	6.25 km × 6.25 km	2002 to 2011	November to April
Willmes and Heinemann (2015b)	MODIS	2 km <sup>2</sup>	2003 to 2015	January to April
Reiser et al. (2020)	MODIS	1 km <sup>2</sup>	2002 to 2021	November to April
Hoffman et al. (2021)	MODIS	1 km <sup>2</sup>	2002 to 2022	November to April
	VIIRS	1 km <sup>2</sup>	2011 to 2022	November to April

Section 2 Data could be changed to “Data and pre-processing”, i.e. to include all data processings before analyses and lead detection method development, e.g. move Section 3.1 (Pre-processing of TIS data) to Section 2.

Detailed descriptions of TIS instrument and its data should moved from Introduction to Section 2.1. In the following are some questions on the TIS data:

What is the size of the TIS image along track?

What is the main intended application of the band 1?

What is the resolution of the TIS data in K?

Is there yet IST product from bands 2 and 3? Under development?

Are there any TIS cloud masking algorithms or products?

**Response:** In accordance with your suggestions, we amended the data presentation and pre-processing sections (please refer to the revised version if the editor decides the manuscript can be revised). We would like to answer your questions about the TIS data here (and have added these details where appropriate in the revised manuscript).

- For convenient use of the TIS data, the ground segment crops the original TIS data to 300 km in the along-track dimension.
- TIS B1 band is a wide channel with a wavelength of 8.0-10.5  $\mu\text{m}$ . It is mainly used in combination with the B2 (10.3-11.3  $\mu\text{m}$ ) and B3 (11.5-12.5  $\mu\text{m}$ ) bands to obtain a better accuracy in land surface temperature retrieval based on the three-channel split-window algorithm (Liu et al., 2021; Hu et al., 2022).

Hu, Z., Zhu, M., Wang, Q., Su, X., and Chen, F.: SDGSAT-1 TIS Prelaunch Radiometric Calibration and Performance, *Remote Sensing*, 14, 4543, 10.3390/rs14184543, 2022.

- Strip noise is a sharp fluctuation in signals that occurs when imaging a homogeneous surface due to different noise bias given by each detector. In general, the TIS B1 band has relatively less strip noise. We have added this to Section 2.2.
- The quantization bit of the TIS is 12 bit. The TIS radiometric measurement is better than 0.42 K for the three bands, which satisfies the preflight requirements ( $\leq 1$  K)
- There are currently no TIS-based surface temperature products or cloud mask products available, all of which are under development.

BTA threshold for the lead detection was manually selected (here 1.8 K). Are you sure this is really applicable for a large amount of TIS images acquired in various sea ice and atmospheric conditions? Why did you not develop an automatic selection method for the BTA threshold, as you did for the BT threshold? I think is rather serious potential flaw in your lead detection method. You should really have an automatic BTA threshold selection method.

**Response:** We did consider using iterative thresholds for the BTA data as well, as Willmes and Heinemann (2015a) did. However, it is hard to argue that automatically selected thresholds are more appropriate than fixed thresholds for few cases in this study. For the three bands lead detection, without the use of a fixed BTA threshold for standard, the comparability of binary segmentation results would be poor, and the further cross-comparisons between the three results would be meaningless.

Although the TIS data used in this study cannot yet include various sea ice and atmospheric conditions, we would like to explain here the soundness of the constant threshold. We tested the results of the threshold values selected by the iterative method. Setting the initial threshold as 1.2 K, the automatically selected BTA thresholds by iterative method for the seven TIS data (for the each of the three bands) were shown in Table R2. The iteration thresholds for the BTA images were relatively close, with the minimum of 1.8 K and the mean of 2.0 K. From this perspective, no large errors can be produced between the segmentation results from iterative selection or from the constant threshold.

Table R2 BTA iteration thresholds for three bands based on seven TIS data

<b>B1</b>	1.9	2.2	1.9	2.2	2.0	1.9	2.5
<b>B2</b>	1.8	2.1	2.1	2.0	2.0	2.0	1.8
<b>B3</b>	1.8	2.1	2.0	1.9	1.9	2.0	2.4

In general, we could have better reliability on your TIS lead detection method if more TIS data had been used in its development. Can you add more TIS images to your study?

**Response:** Although we would like to carry out more detections, what we have presented in this manuscript is all that can be done in the spring of 2022. On the one hand, the SDGSAT-1 was launched just one year ago, so we can only obtain data after March 2022. On the other hand, the cloud interference is the main limitation for lead

detection based on thermal infrared data in the Arctic. Due to the unavailability of simultaneous cloud detection (we are also working on this point), the method proposed in this study is only concerned with clear sky conditions, and therefore the available data is limited.

While it is possible to collect the TIS data for the winter from 2022 to 2023, it is expected that there will be differences in detection performance between seasons. The aim of this study is to demonstrate the feasibility of the SDGSAT-1 TIS, a new 30 resolution sensor, for lead detection. Thus, despite the limited data, our results suggests that the TIS is competitive and promising for application in Arctic lead observations.

Currently, SDGSAT-1 needs to take into account various imaging requirements in different areas, so it is difficult for the satellite to keep observing the polar regions for long periods. The SDGSAT-1 data over the Arctic are still ongoing collected. Besides, the three payloads of SDGSAT-1 (TIS, Glimmer Imager for Urbanization (GIU) and Multispectral Imager for Inshore (MII)) allow for daytime and nighttime atmosphere monitoring capabilities. The corresponding SDGSAT-1 cloud product is under development.

The TIS lead map is evaluated against the Sentinel-2 lead map, and their agreement is very high, 96.3%. You talk about accuracy of the TIS lead map based on this comparison, but this comparison really don't give an absolute accuracy of the TIS map, as I don't think your Sentinel-2 lead map is error free. For determination of accuracy in-situ or airborne data are needed.

**Response:** We agreed with you that it would be more valuable to compare in-situ and airborne measurement. For example, the recent 1 m resolution IST data based on flight-borne thermal infrared camera in the MOSAIC expedition is interesting (Thielke et al., 2022), while this dataset only covers the central Arctic. Field data is, after all, scarce and hard to match with our SDGSDA-1 TIS data, and supposedly are well beyond the scope of this study.



In terms of validation of the accuracy of lead detection, previous studies based on moderate resolution thermal infrared remote sensing have also used a variety of different methods. For example, Willmes and Heinemann (2015) used the normalized brightness images derived from MODIS near-infrared (NIR) data (channel 2, 841–876 nm) with a resolution of 250m × 250m for validation. Hoffman et al. (2019) compared their time-series results with the Willmes and Heinemann (2015). Hoffman et al. (2021) used the masks derived from hand analysis as a proxy for validation in the absence of ground truth in the Arctic and conducted a comparison with the legacy product by Hoffman et al. (2019). Qu et al. (2021) used three successive Landsat-8 NIR images at 30 m resolution to assess the accuracy of their lead detection. As for other lead detection studies, Murashkin and Spreen (2018) evaluated the S1-derived lead results in comparisons with S2 optical satellite data. But instead of assigning reflectance thresholds to the S2 data, they manually marked the S1 data by overlaying the S2 image to confirm the validity of leads.

Overall, even with certain errors, it is sound to use S2 data with normalized brightness and objective companions for validation in this study.

TIS strip noise is discussed first time under Results. It should be mentioned when TIS sensor and data properties are described under Section 2.

It would be very interesting see lead map comparison between TIS (30 m) and Landsat (100 m), can you add this to your paper? We could see how much 30 vs. 100 m resolution matters in the lead detection.

Finally, under ‘Summary and conclusion’ Section you discuss more about future research goals, and will be there an operational TIS lead product?

**Response:** Landsat-8 at 100 m resolution is indeed appropriate to be used for comparison with the TIS results. However, we did not acquire the matched Landsat-8 data during SDGSAT-1 TIS imaging. So, we only compared with the MODIS data at 1km resolution. The figure below shows the coverage of Landsat-8 in the Beaufort Sea on 3 April 2022 (available on the United States Geological Survey website,

<https://www.usgs.gov/>).

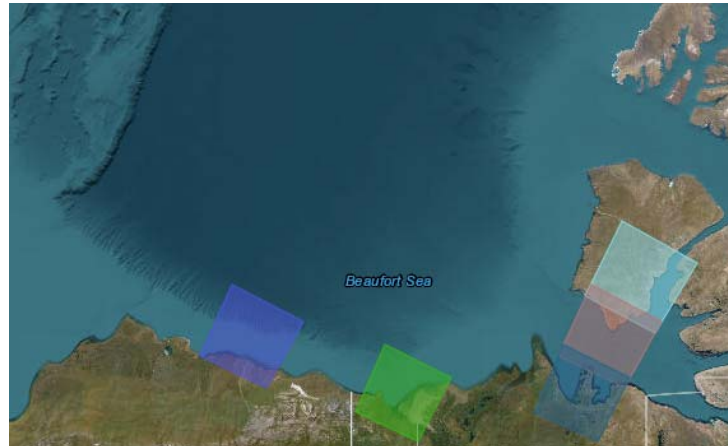


Figure R1 The search result for Landsat-8 in the Beaufort Sea on 3 April 2022 (<https://www.usgs.gov/>)

In the future, we do plan to develop a long-term lead dataset based on SDGSAT-1 TIS at 30 m resolution to support relevant research about sea ice dynamic, which requires more SDGSAT-1 data accumulation and development of related products (particularly cloud products and surface temperature products).

## Specific comments

### Abstract

“unresolvable ice leads”; change to “unresolvable sea ice leads” or to “unresolvable leads”

**Response:** Done as it is suggested.

### 1. Introduction

line 28: “under wind and water stresses” better “under wind and ocean stresses”.

**Response:** Done as it is suggested.

l. 33: “During winter, newly opened leads are the main source of ice production, brine rejection, and turbulent heat loss to the atmosphere”

Is it leads or polynyas in the whole Arctic scale? Please check. Anyway polynyas could be mentioned in this context.

**Response:** Done as it is suggested. The sentence is modified “During winter,

newly opened leads and polynyas are the main source of ice production, brine rejection, and turbulent heat loss to the atmosphere”

l. 47: “Other studies also applied active and passive microwave data to lead detection with the advantage that microwave wavelengths are transparent to cloud cover; however, either the data resolution is too coarse”

Too coarse to what? Detect smaller leads? In some application of the lead data?

**Response:** The “coarse resolution” here meant that the leads derived from AMSR-E with a resolution of 6.25 km is coarser than the moderate resolution thermal infrared (with resolutions of hundreds of or thousands of meters) and high-resolution optical images (tens of meters of resolution). Some studies shown that the 6.25 km resolution lead dataset is not ideal for the evaluation of narrow leads. Ólason et al. (2021) used the AMSR-E lead dataset developed by Bröhan and Kaleschke (2012a) to evaluate the ability of a new sea ice model in reproducing lead characteristics. They found that “small leads are known not to be captured by the AMSR-E because of its resolution limitation”. Including, but not limited to, Ivanova et al. (2016) applied SAR data to assess the error in the AMSR-E lead dataset and found a consistent overestimation of lead fraction by a factor of 2 to 4 in the AMSR-E product.

Ivanova, N., Rampal, P., and Bouillon, S.: Error assessment of satellite-derived lead fraction in the Arctic, *The Cryosphere*, 10, 585–595, <https://doi.org/10.5194/tc-10-585-2016>, 2016.

l. 57: “Essentially, IST data, which are generally retrieved by the split-window technique (Key et al., 1997), are less accurate under the presence of melt ponds and leads because the lower emissivity (0.96 compared to 0.99) can cause a difference in the retrieved temperature”

Lower emissivity of what? Water?

**Response:** Since melt ponds and leads contain water, they have lower emissivity than that of snow or ice, say 0.96 compared to 0.99. Please refer to Key et al. (1997) and Hall et al. (2001) for details. The sentence is revised “because the lower emissivity (0.96 compared to 0.99) of water than sea ice”.

l. 61: “They detected leads for January through April over the period of 2003 to 2018, presenting a lower estimation for the lead area compared with the results in Willmes and Heinemann (2015c); the reason is the difference in spatial resolutions of the lead datasets.”

Give resolutions of these datasets in the text.

**Response:** We have modified this to “the reason is the difference in spatial resolutions of the lead datasets (1 km compared to 2 km)”.

l. 67: “Qu et al. (2021) proposed a modified algorithm Modified from what? From Hoffman et al?”

**Response:** The sentence is revised “Qu et al. (2021) proposed a modified algorithm from Willmes and Heinemann (2015a) to detect daily spring leads in the Beaufort Sea based on the IST data retrieved from MODIS swath products”.

l. 94: “To date, the TIS has acquired substantial high-resolution thermal infrared data from the critical seas in the Arctic”

How do you define what is a critical area in the Arctic? Explain in the text.

**Response:** In the scope of this study, the critical seas refer to areas pervaded by leads with significant sea ice dynamic process.

Wernecke and Kaleschke (2015) showed that the lead fraction in Baffin Bay, the Fram Strait region, the northern Barents Sea, the Kara Sea, the western Laptev Sea and the Chukchi Sea are commonly up to around 15 %. In the southern Beaufort Sea and especially its shear zone next to the coastline, lead fraction values are up to 6 %. A strong lead divergence and opening processes were observed in the Beaufort Sea (Beitsch et al., 2014). The model simulation by Wang et al. (2016) also suggested that winter ice leads are mainly formed in marginal seas (Barents, Kara, Laptev, and Beaufort Seas) and near Fram Strait. In particular, leads fraction in the Beaufort Sea shows a significant interannual variability.

Thus, the Beaufort Sea and Laptev Sea can be considered to as the critical areas for lead observation.

Beitsch, A., Kaleschke, L., and Kern, S.: Investigating high-resolution AMSR2 sea ice concentrations during the February 2013 fracture event in the Beaufort Sea, *Remote Sensing*, 6, 3841-3856, 2014.

Wang, Q., Danilov, S., Jung, T., Kaleschke, L., and Wernecke, A.: Sea ice leads in the Arctic Ocean: Model assessment, interannual variability and trends, *Geophysical Research Letters*, 43, 7019-7027, 2016.

1. 102: “This study is the first to observe Arctic sea ice leads at 30 m resolution”

**Response:** This has been modified to “This study focuses on observing Arctic sea ice leads based on spaceborne thermal infrared remote sensing at 30 m resolution and reveals more details than the moderate-resolution thermal infrared sensors.”

Table 1 must include references to the data it present.

**Response:** Agree. The reference is:

International Research Center of Big Data for Sustainable Development Goals (CBAS): SDGSAT-1 Data Users Handbook (Draft), 2022. <http://60.245.209.56/preview/20221125/c84c0b5d89984cd384ffa05dbb163d14.pdf>

Figure 1 should include acquisition times for the rectangles 1-4. Describe that visible images come from Sentinel-2.

**Response:** We have added corresponding dates and descriptions to the notes of Figure 1: “The black borders mark four successive groups of cloudless images (group 1 was acquired on 3 April, group 2 on 28 April, groups 3 and 4 on 23 March)”. Please refer to the Table 2 in the original manuscript for more details of data information.

## **2. Data**

1. 130: “Considering the benefit of incorporating three thermal infrared bands for observation, Thus, the three bands of SDGSAT- 1 TIS data are used”

You can remove ‘thus’ from the sentence.

**Response:** Done as it is suggested.

1. 131: “The georeferenced level-4 TIS data”

What do you mean by level-4 data here?

**Response:** The SDGSAT-1 data products include different Level-1, Level-2 and Level-4 data products. Level-1 product is a standard product based on the Level-0 product, after data processing such as relative radiometric correction, band registration, HDR fusion, etc. Level-2 product is based on the Level-1 product after geometric correction. Level-4 product is based on the Level-1 product after ortho-rectification using ground control points and Digital Elevation Model (DEM) and output with standardized format. Currently, only Level-4 product is available to

users (CBAS, 2022).

Give some references to Sentinel- 1 and -2 sensors and data.

**Response:** Done as it is suggested. The User Guides for S1 and S2 are cited as references:

European Space Agency (ESA): Sentinel-1 User Handbook, 2013.

European Space Agency (ESA): Sentinel-2 User Handbook, 2015.

l. 139: “given that the visible spectrum centered at 560 nm gives a good effect (König et al., 2019) for a scene containing sea ice and seawater. ”

What is this ‘effect’? Good discrimination between sea ice and water?

**Response:** We visually compared S2 visible images (bands 2, 3 and 4) and found good discrimination between leads and surrounding sea ice from the band 3. Therefore, it is appropriate to use the S2 green band images as the reference for validation.

l. 147: “we collected S1A dual-polarization data in the Beaufort Sea on April 3 and 28, 2022 (see Table 2).

Table 2 shows S- 1 data only on 3 Apr.

**Response:** We have corrected this in the revised version. It should be “we collected S1A dual-polarization data in the Beaufort Sea on April 3 in 2022”.

Table 2: S-1 resolution is not 40 m, it is around 100 m, the pixel size is 40 m. Explain what are h07/08 etc. under MODIS column.

**Response:** Thanks for pointing these out. We have changed the information about S1 data. It should be “pixel size: 40 m” for the Sentinel-1 EW data.

For the level-3 MOD29 product, “hxx” and “vxx” are the horizontal tile number and vertical tile number of product. We have taken on the advice of reviewer 1 and conducted the experiment using the level-2 MOD29 product. The level-2 MOD29 data information are listed in Table R3.

Table R3 Information of MODIS products used in this study

		MOD29	MOD03
Date and time (UTC)	2022-03-23	10:30	10:30
		12:05	12:05
	2022-04-03	05:10	05:10
		05:05	05:05
Spatial resolution		1 km	1 km

l. 163: “air temperature) data available by every 6 hours” Your ERA5 reference shows that data is hourly.

**Response:** We have corrected this. It should be “The ERA5 near-surface air temperature (2 m air temperature) data is available hourly in a regular grid of 0.25 degrees.”

OMI ozone: give some reference also for the ozone retrieval, in addition to the product reference.

**Response:** Agree. The literature about ozone retrieval is cited, with the corresponding description: “The total column ozone is retrieved based on the long-standing TOMS V8 retrieval algorithm (Bhartia, 2002), which uses a weakly absorbing wavelength (331.2 nm) to estimate an effective surface reflectivity and another wavelength (317.5 nm) with stronger ozone absorption to estimate ozone.”.

Bhartia, P. K.: OMI Algorithm Theoretical Basis Document, Volume II, OMI Ozone Products, Greenbelt, Maryland, USA, NASA Goddard Space Flight Center 2002.

### **3. Method**

l. 195: “In addition to the leads presenting as distinct yellow and red colors on the BT map, Give also temperature ranges these colors represent.

**Response:** The sentence was modified to “the leads presenting as distinct yellow and red (in the temperature range of 242 K to 252 K) colors on the BT map”.

Give some references to the BTA based lead detection in Section 3.2, as this method has been used in many studies using MODIS and VIIRS data.

**Response:** Agree. We added relevant references at the beginning of Section 3.2.

“Ice leads containing seawater and thin ice have temperatures higher than the surrounding sea ice. Therefore, the temperature contrast between leads and the sea ice surface is the basis of detecting ice leads (Willmes and Heinemann, 2015a; Hoffman et al., 2019; Qu et al., 2021).”

l. 208: “By collecting eight TIS data acquired between April 3 and April 28” There is seven TIS images in Table 2.

**Response:** Thanks for pointing it out. It should be seven TIS images. We have corrected this in the manuscript.

l. 222: “Previous methods applied a variety of BTA thresholds”

should be “Previous studies”, and give also references.

**Response:** Done. The sentences have been modified “Previous methods applied a variety of BTA thresholds. Hoffman et al. (2019) identified a threshold of 1.5 K. Qu et al. (2021) took 1.2 K, 1.5 K and 2 K as thresholds for different types of leads, corresponding to large to small uncertainty levels.”.

Figure 6 and 7: give TIS band used in the figures.

**Response:** Done as it is suggested. The used SDGSAT-1 TIS data ID (KX10\_TIS\_20220403\_W128.84\_N73.00\_202200033226) is the same as in Figures 4 and 5.

l. 268: “Finally, the binary detection of leads at a 30 m resolution was derived based on SDGSAT- 1 TIS in three bands.”

How all three bands were used together in the lead detection? You must explain this in detail.

**Response:** The TIS data from each of the three bands was fed separately into the detection algorithm, and the outcomes were three binary lead maps. Except for Section 4.3, where we explicitly said that the three results were combined into a lead map, all the rest was based on three results from the three bands. In terms of the detection performance, each band has its advantage on leads detection, so we consequently suggest using the combined results of the leads detected from the three TIS bands.



The sentence is modified “Finally, three binary results at 30 m resolution were derived separately from each of the three bands of the SDGSAT-1 TIS.”.

#### **4. Results**

l. 302: spell out TP, FP, FN and TN in the text,

Done

Section 4.2: equation numbers should be (2) and (3).

Done

Section 4.3: again how lead detections by all three TIS bands are combined?

**Response:** The sentence was modified: “Simultaneously, we combined the three lead maps based on the three TIS bands into one binary map, in which the combined pixel is positive as long as one of the three maps gives a positive pixel. The combined map contains the most leads (see Figure 11 (c)).”

l. 381: “The previously developed method (Qu et al., 2021) was applied to detect the leads based on the MODIS IST data.”

Explain in the text why you selected the method by (Qu et al., 2021).

**Response:** We used the method by Qu et al. (2021) to detect leads from MODIS IST data because it is based on an analogous principle to our proposed method, i.e., both used fixed BTA thresholds for binary segmentation. The use of analogous methods allows for a fair comparison of the differences in lead observations between the two sensors. We have added this to the revised version.

#### **5. Discussion**

You talk in the text about ‘ozone resolution’, what is that? Figure 12 shows ‘best total ozone solution’.

**Response:** It is a typo. It should be the “ozone solution”. We have corrected them.

You could add to the discussion here the correlations between different TIS bands.

**Response:** We have shown cross comparisons of the lead detection results from the TIS three band in Section 4.2. The three bands give highly consistent detection results. The inconsistent lead pixels detected from the three bands account for 11.46%, 23.30%, and 21.88%, respectively. The correlation between the thermal characteristics of the leads for the three bands is evident. Therefore, we did not further discuss this.

Section 5.2: Descriptions on S-1 SAR processing should go to Data Section.

**Response:** Done as it is suggested. The SAR data processing has been amended in Section 2.2: “The dual-polarization data were radiometrically calibrated, and a false-color composition was performed by assigning the HH, the subtraction of HH by HV and the HV images to the red, green and blue channels, respectively.”

1. 483: “In particular, the B2 band is more sensitive to such surface information because various types of sea ice have different emissivity and produce different BT values.”

Are the TIR emissivities of different sea ice types really that different? Please check literature, and give variation range in the text. I would say it is more about variation of sea ice/snow surface temperature, e.g. thin sea ice has surface temperature which is a function of freezing temperature and air temperature, but surface of thick ice is fully insulated from ice bottom, i.e. only air temperature matters.

**Response:** Thanks very much for your valuable comment. We have reviewed the relevant literatures. Indeed, as you say, TIR (thermal infrared) emitted energy mainly reflects the skin radiometric information of the ice/ snow. It is a function of surface temperature and emissivity, also influenced by meteorological conditions.

For TIR wavelength region, water emissivity is stable, about 0.96. Snow and ice have high emissivity, but with variations (Sandven and Johannessen, 2006). Theoretically, the emissivity of ice/snow decreases with increasing grain size and increasing density, enhancing the emissivity spectral contrast (Warren, 2019). Ice/snow type dependent emissivity can produce a brightness temperature difference. Laboratory measurements of terrestrial material emissivities indicate that snow/ice emissivity changes spectrally with snow/ice conditions such as grain size and packing fraction (Tonooka and Watanabe, 2005). The field measurement shows that the emissivity of fine-grained snow is very high for the nadir angle, 0.997 and 0.984 for

10.5  $\mu\text{m}$  and 12.5  $\mu\text{m}$ . The emissivities of coarse-grained snow are 0.995 and 0.971, and become sensitive to viewing angle. The emissivity of bare ice is the lowest, 0.993 and 0.949 for 10.5  $\mu\text{m}$  and 12.5  $\mu\text{m}$ , respectively, with the largest angular dependence (Hori et al., 2006; Hori et al., 2013). Additionally, due to the mixed pixel effect in TIR remote sensing, the presence of unresolved melt ponds and leads can also change the surface emissivity (Hall et al., 2001).

Nevertheless, the differences in the ice/snow surface emissivity in the TIR spectra above mentioned are small. The effect of mixed pixels is also small, especially for the fine scales of focus in this study. In contrast, ice/snow thickness can vary significantly over short distances and on ice of different ages. The morphology of the snow cover, in conjunction with the air temperature near the surface, can be expected to be a significant cause of surface temperature variations (Poulin, 1975).

Hence, as you say, the variations in BT values for the SDGSAT-1 TIS in this study is more likely to be caused by ice/snow surface temperatures. For thin ice, its surface temperature is close to the temperature of surrounding icefree water and underside water depending on the thickness. For thick ice, it is covered by snow and insulated from ice bottom, so its surface temperature is generally close to that of surface air temperature (Comiso et al., 2019).

Thielke et al. (2022) obtained sea ice surface temperatures at 1 m resolution based on helicopter-borne thermal infrared images in the MOSAiC expedition during winter 2019/2020. The high-resolution temperature images show significant warmer line features, i.e., opened leads, with internal surface temperature variability. They also found the high variability of surface temperature for surrounding sea ice at high resolution, and explained it as the result of difference ice thicknesses. This temperature variation characteristic is similar to the situation we described in our Figure 13 and therefore supports our analysis.

The corresponding paragraph has been amended: “contours of multiyear ice with high backscatter values that are observed in SAR images are similar to some negative

BTA features... This suggests surface temperature variations for different thicknesses of sea ice. Similar surface temperature variations are also found in the 1 m resolution IST data derived from helicopter-borne thermal infrared imaging (Thielke et al., 2022).”.

Poulin, A. O.: Significance of surface temperature in the thermal infrared sensing of sea and lake ice, *Journal of Glaciology*, 15, 277-283, 1975.

Sandven, S. and Johannessen, O. M.: Sea ice monitoring by remote sensing, 2006

Hori, M., Aoki, T., Tanikawa, T., Motoyoshi, H., Hachikubo, A., Sugiura, K., Yasunari, T. J., Eide, H., Storvold, R., and Nakajima, Y.: In-situ measured spectral directional emissivity of snow and ice in the 8–14  $\mu\text{m}$  atmospheric window, *Remote Sensing of Environment*, 100, 486-502, 2006.

Hori, M., Aoki, T., Tanikawa, T., Hachikubo, A., Sugiura, K., Kuchiki, K., and Niwano, M.: Modeling angular-dependent spectral emissivity of snow and ice in the thermal infrared atmospheric window, *Applied optics*, 52, 7243-7255, 2013.

Tonooka, H. and Watanabe, A.: Applicability of thermal infrared surface emissivity ratio for snow/ice monitoring, *Multispectral and Hyperspectral Remote Sensing Instruments and Applications II*, 282-290, 2005

Warren, S. G.: Optical properties of ice and snow, *Philosophical Transactions of the Royal Society A*, 377, 20180161, 2019.

Josefino C. Comiso, Dorothy K. Hall, and Rigor, I.: Ice Surface Temperatures in the Arctic Region, in: *Taking the Temperature of the Earth*, edited by: Glynn C. Hulley, and Ghent, D., Elsevier, 10.1016/B978-0-12-814458-9.00005-8., 2019.

Thielke, L., Huntemann, M., Hendricks, S., Jutila, A., Ricker, R., and Spreen, G.: Sea ice surface temperatures from helicopter-borne thermal infrared imaging during the MOSAiC expedition, *Scientific Data*, 9, 364, 10.1038/s41597-022-01461-9, 2022.

l. 498: “On the other hand, as the TIS data available within the scope of this paper is relatively limited, these individual case studies presented may be weak in terms of generalizability.”

Yes, this is the case, and this must be also emphasized in Conclusion Section.

**Response:** We agree with you about the limitations of this study. We have mentioned it in the Conclusion Section: “Nevertheless, limited by the imaging time and cloudy conditions over the Arctic region, only individual case studies based on TIS data were carried out.”.

## Technical corrections

Many figures are too small, try to increase their sizes. Also colorbars for BT, BTA, are way too small.

References for the same authors and the same year are missing a,b,c, after the year in Reference list.

**Response:** Thank you very much for your detailed advice. We will improve the quality of these figures and check the citation format of the literatures.